Band bending and surface defects in β-Ga2O3

T. C. Lovejoy, Renyu Chen, X. Zheng, E. G. Villora, K. Shimamura, H. Yoshikawa, Y. Yamashita, S. Ueda, K. Kobayashi, S. T. Dunham, F. S. Ohuchi, and M. A. Olmstead

Citation: Applied Physics Letters **100**, 181602 (2012); doi: 10.1063/1.4711014
View online: http://dx.doi.org/10.1063/1.4711014
View Table of Contents: http://scitation.aip.org/content/aip/journal/apl/100/18?ver=pdfcov
Published by the AIP Publishing

Band bending and surface defects in β-Ga_2O_3

T. C. Lovejoy,[1,2,a)] Renyu Chen,[2,3] X. Zheng,[2,4] E. G. Villora,[5] K. Shimamura,[5] H. Yoshikawa,[6] Y. Yamashita,[6] S. Ueda,[6] K. Kobayashi,[6] S. T. Dunham,[2,3] F. S. Ohuchi,[2,4] and M. A. Olmstead[1,2]

[1]*Department of Physics, University of Washington (UW), Box 351560, Seattle, Washington 98195, USA*
[2]*Center for Nanotechnology, UW, Seattle, Washington 98195, USA*
[3]*Department of Electrical Engineering, UW, Box 352500, Seattle, Washington 98195, USA*
[4]*Department of Materials Science and Engineering, UW, Box 352120, Seattle, Washington 98195, USA*
[5]*National Institute for Materials Science, 1-1 Namiki, Tsukuba 305-0044, Japan*
[6]*NIMS Beamline Station at SPring-8, National Institute for Materials Science, Hyogo 679-5148, Japan*

(Received 2 October 2011; accepted 14 April 2012; published online 2 May 2012)

Surface band bending and surface defects on the UV-transparent conducting oxide β-Ga_2O_3 (100) are studied with hard x-ray photoemission spectroscopy and scanning tunneling microscopy. Highly doped β-Ga_2O_3 shows flat bands near the surface, while the bands on nominally undoped (but still *n*-type), air-cleaved β-Ga_2O_3 are bent upwards by $\gtrsim 0.5$ eV. Negatively charged surface defects are observed on vacuum annealed β-Ga_2O_3, which also shows upward band bending. Density functional calculations show oxygen vacancies are not likely to be ionized in the bulk, but could be activated by surface band bending. The large band bending may also hinder formation of ohmic contacts. © *2012 American Institute of Physics*. [http://dx.doi.org/10.1063/1.4711014]

Wide-band-gap oxides, such as Ga_2O_3, In_2O_3, SnO_2, ZnO, and their alloys, are of key importance as transparent conductors and gas sensing materials. β-Ga_2O_3 has the largest band gap of these oxides (4.5–4.8 eV).[1] The typical *n*-type conductivity in Ga_2O_3 is commonly attributed to oxygen vacancies due to an inverse correlation between the conductivity and the oxygen pressure $p(O_2)$ during growth,[2] and by extension from other oxides.[3] A recent experimental study challenges this model by showing the Si impurity level in commercially available source materials is sufficient to account for the observed *n*-type conductivity,[4] and a recent theoretical study shows the oxygen vacancy to be a deep donor, while Si and H lead to *n*-type conductivity.[5] However, while Si-doping can increase the conductivity of Ga_2O_3, this does not explain its dependence on $p(O_2)$, which is convincingly demonstrated for Ga_2O_3 in a gas sensing device. Bartic *et al.*[6] demonstrated a few percent change in the conductivity of a single crystal device at 1000 °C due to changes in $p(O_2)$; for the single crystal sensor, the active region was found to be confined to a narrow region near the surface.

This letter reports on surface band bending and defects in pure and highly silicon-doped β-Ga_2O_3 (100). High kinetic energy x-ray photoemission spectroscopy shows the bands of pure Ga_2O_3 are bent upwards by at least 0.5 eV at the surface, indicating a negative charge on the surface. Negatively charged surface defects are observed with scanning tunneling microscopy (STM) on nominally undoped samples after annealing in vacuum, a process that also increases upward band bending. Density functional theory (DFT) calculations of oxygen and gallium vacancies on different sites show neither vacancy type is consistent with persistent conductivity in high purity samples. The activation energy for oxygen vacancies to donate electrons to the conduction band is at least 0.35 eV, making their excitation in bulk Ga_2O_3 unlikely, but raises the possibility of a near-surface excitation layer when the bands are bent upwards. The observed band bending may also explain the difficulty in making ohmic contacts to Ga_2O_3.

Hard x-ray photoemission spectroscopy (HXPS, $h\nu = 5953.4$ eV) was performed at BL15XU of SPring-8 in Japan. Single crystal samples were taken from the end points in a study[4] showing the control of carrier concentration with Si doping from 5×10^{16} cm^{-3} for the purest sample (6N $\equiv$ 99.9999% pure starting materials) to 2×10^{18} cm^{-3}. The surface depletion region is then ~50 nm for the "pure" crystal and ~7 nm for the doped crystal.[7] HXPS samples were cleaved in air and quickly inserted into ultrahigh vacuum (UHV) for measurement. A 10 kV-R4000 Scienta energy analyzer captured photoelectrons in a $\sim \pm 7°$ angular window centered 90° from the incident photon direction.

STM and soft XPS (monochromatized Al K α, $h\nu = 1486.7$ eV) were performed in Seattle on nominally undoped β-Ga_2O_3 samples from 4N (99.99% pure) starting materials, which results in conductivity sufficient for STM. STM samples were prepared by prolonged direct-current heating in UHV to 800–1000 °C, as in Ref. 8.

DFT calculations employed the Vienna *Ab-initio* Simulation Package (VASP) (Ref. 9) with the generalized gradient approximation (GGA).[10] Ultra-soft pseudo potentials[11] were used with 6 valence electrons for oxygen, and 13 for gallium. All calculations were done in a 160 atom cell ($1\vec{a} \times 4\vec{b} \times 2\vec{c}$ or $\sim 12 \times 12 \times 12$ Å^3) using a $2 \times 2 \times 2$ Monkhorst-Pack *k*-point sampling.

Near-surface band bending on β-Ga_2O_3 (100) was probed through both angle and photon-flux dependent measurements of Ga $2p_{3/2}$ and O 1*s* emission. Low-emission-angle spectra are dominated by near-surface emission and reflect the band position close to the surface, while high-angle (near-normal) spectra integrate over the ~7 nm escape depth.[12] If the bands are bent in the dark, photoexcited carriers screen the near-surface field and "flatten" the bands,[13]

[a)]Electronic address: tlovejoy@uw.edu. Present address: Nion Co., 1102 8th St., Kirkland, WA 98033, USA.

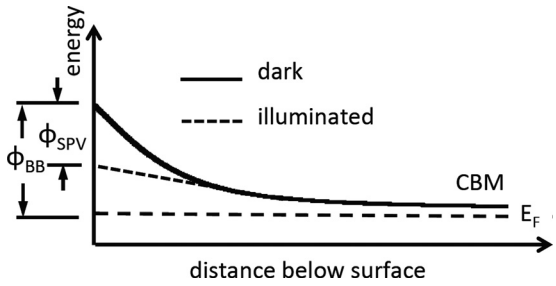

FIG. 1. Schematic band diagram showing surface band bending with magnitude ϕ_{BB} (dark conditions, solid line) and surface photovoltage ϕ_{SPV} (illuminated conditions, dashed line) on the binding energy of the conduction band minimum at the surface of an *n*-type semiconductor. Since the surface is not reconstructed, see Ref. 8, the Ga 2*p* and O 1*s* peaks track the valence and conduction band edges.

resulting in a variation of binding energy with photon flux, or surface photovoltage (SPV) (see Fig. 1).

Figure 2 shows the HXPS Ga $2p_{3/2}$ binding energy from "Si-doped" and "6 N" samples as a function of photon flux ($\theta_e = 88°$); O 1*s* energies at an intermediate flux level are also shown. Emission from the Si-doped sample shifts by less than 0.01 eV over the available range of photon flux. In the 6N sample, the peak position varies weakly at high flux, but shifts sharply toward lower binding energy as the photon flux decreases. At high flux, the energy difference between the peak positions in the doped and 6N samples is 0.355 ± 0.003 eV for Ga $2p_{3/2}$ (solid symbols) and O 1*s* (open symbols) and for the valence band maximum (data not shown). Linear extrapolation of the two lowest intensity points to zero flux yields a difference in Ga $2p_{3/2}$ peak positions in the two samples of ~ 0.52 eV, which, as discussed below, is a lower limit to the band bending. With soft XPS (low flux and high surface sensitivity), 4N β-Ga_2O_3 shows O 1*s* binding energies ~ 0.2 eV less than for Si-doped, decreasing an additional 150 mV upon high temperature annealing.

For the highly doped sample, where the electron inelastic scattering length is comparable to the expected band-bending length scale (~ 7 nm) and no SPV shift results from the flux variation with angle, both the Ga $2p_{3/2}$ and O 1*s* emission energy remained constant within ± 50 meV as the emission angle varied from 15° above grazing (probe depth ~ 2 nm) to 88° (near-normal). The peak widths also remained essentially constant.

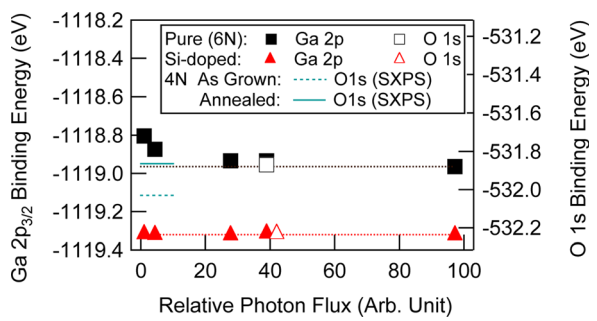

FIG. 2. Dependence of Ga $2p_{3/2}$ core level peak position on photon flux (normalized to highest measured flux) for "6N" (squares) and "Si-doped" (triangles) β-Ga_2O_3. HXPS O 1*s* binding energies for a single flux are shown as open symbols. Short lines are soft XPS O 1*s* binding energies for a 4N sample before (dashed line) and after (solid line) annealing.

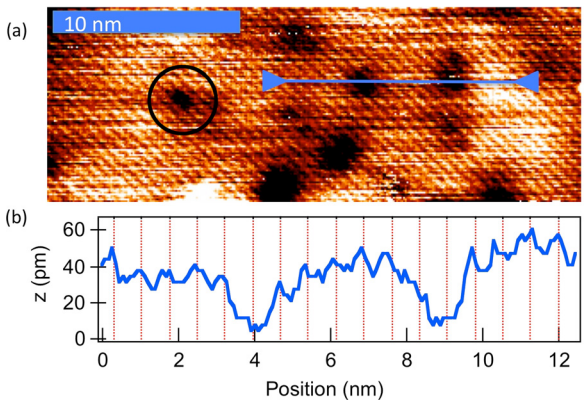

FIG. 3. (a) Atomic resolution STM image showing atomic corrugation along *c* direction (diagonal lines) and several surface defects (dark spots). One such defect is emphasized with a black circle. (b) Line profile (along the blue line marked with arrows) through two defects in (a). Lines in (b) are spaced 0.73 nm ($=c_o/\tan(52°)$). (10 nm scale bar, empty-state STM conditions: +7 V on sample.)

Atomic scale defects at the β-Ga_2O_3 (100) surface were studied with STM to investigate possible origins of the surface charge associated with the observed band bending. Figure 3(a) shows several defects (dark in this empty state image) on an atomically flat terrace with "B" termination; the regularly spaced diagonal rows correspond to the atomic corrugation in the *c* direction.[8] Figure 3(b) shows an apparent-height profile through two defects along the line between the arrows in (a). The defects cause ~ 0.4 Å deep, 1.3 nm wide depressions centered on the flat, regular atomic rows.

The bulk formation energy of a defect is a fundamental quantity in determining its equilibrium abundance in a material. The formation energy, E^f, of a vacancy defect of atom *x* with charge state *q*, V_x^q, was calculated with DFT:GGA using[14]

$$E^f(V_x^q) = E_{tot}(V_x^q) - E_{tot}(Ga_2O_3) + qE_F - n_O\mu_O - n_{Ga}\mu_{Ga}, \quad (1)$$

where E_{tot} (Ga_2O_3) and E_{tot} (V_x^q) are the total energies of the relaxed structures with no defects and with the charged vacancy, V_x^q, respectively. E_F is the electron chemical potential, which is also called the Fermi level. n_x is the number of atoms of type *x* that have been removed to form the vacancy, and μ_x the chemical potential for species *x*. The transition level $\varepsilon(q/q')$ is the Fermi level where $E^f(V_x^q)$ is equal in the two charge states (for a review, see Ref. 14).

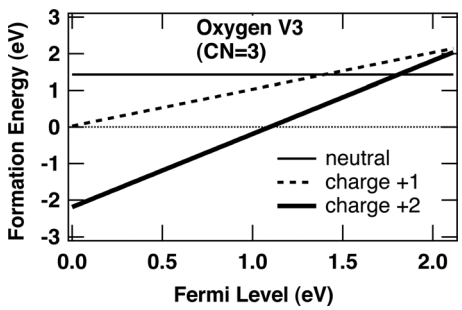

FIG. 4. Formation energy of oxygen vacancy defect V_{O3} under gallium rich conditions as a function of Fermi level for each charge state: neutral (thin solid line), +1 (dashed line), and +2 (thick solid line).

The β-Ga_2O_3 crystal structure has three distinct oxygen sites and two gallium sites: O_1 and O_3 each have three Ga neighbors, and O_2 has four; Ga_1 is tetrahedral (4 neighbors) and Ga_2 is octahedral (6 neighbors).[15] Fig. 4 shows the computed formation energies (under Ga rich conditions, $\mu_{Ga} = -2.94\,\text{eV}$) for the O_3 vacancy (1 Ga_2 and 2 Ga_1 neighbors) as a function of E_F position within the DFT:GGA gap (2.13 eV) for each of three possible charge states: $q = 0$, $+1$, and $+2$. The calculated formation energies and transition energies for vacancies on the five distinct sites are in Table I.

For all three oxygen sites, the charge state with the lowest formation energy is the doubly ionized V_O^{2+} in *p*-type material, and the neutral V_O^0 in *n*-type material. Singly ionized oxygen vacancies never have the lowest formation energy. The four-fold V_{O2}^0 has the lowest formation energy $[E^f(V_{O2}^0) = 0.71\,\text{eV}]$ of the three neutral oxygen vacancies and, hence, the lowest formation energy of all sites and charge states for n-type β-Ga_2O_3; its $\varepsilon(2^+/0)$ transition level is near mid-gap (1.1 eV). The transition levels for the 3-fold vacancies are closer to E_c; V_{O3} has the smallest activation energy, $E_c - \varepsilon(2^+/0) = 0.32\,\text{eV}$, although image charge corrections (not included here) would increase this value.

Under Ga-rich conditions, $E^f(V_{Ga1}^0)$ and $E^f(V_{Ga2}^0)$ are much higher than $E^f(V_O)$, although they are comparable under O-rich conditions (see Table I). For *p*-type β-Ga_2O_3, the neutral tetrahedral site vacancy has lowest energy, while in the *n*-type system, the octahedral V_{Ga2}^{3-} is the most stable.

The above results may be summarized as follows: the bands in highly *n*-doped, air-cleaved β-Ga_2O_3 are essentially flat within a few nm of the surface, while high purity air-cleaved β-Ga_2O_3 shows a SPV indicating at least 0.5 eV upward band bending. Air-cleaved 4 N β-Ga_2O_3 shows a similar band bending that increases by 150 mV upon annealing in UHV. Annealing in UHV leads to accumulation of surface point defects that appear as depressions in empty state images, which are centered on the elevated surface rows. Calculations show oxygen vacancies are not ionized in *n*-type material with a Fermi level near E_c, and the minimum DFT:GGA activation energy for carrier production (> 0.32 eV) is much larger than k_BT (~ 0.03 eV).

Direct comparison of the peak positions in doped and pure Ga_2O_3 requires information on the relative alignment of the bulk bands and Fermi level. The effective mass at the conduction band minimum (CBM) is calculated by Varley *et al.* to be $0.28m_o$,[5] leading to a CB density of states $N_c \sim 4 \times 10^{18}\,\text{cm}^{-3}$. Fermi statistics would then place the Fermi level about 10 meV below the CBM for the 6 N sample, with $n \sim 5 \times 10^{16}\,\text{cm}^{-3}$, and above the CBM for the highly doped sample. However, optical measurements of Si-doped β-Ga_2O_3 indicate the overlapping donor orbits form an impurity band roughly 0.06 eV below the CBM,[16] which would pin E_F there. In any case, the bulk Fermi levels in the 6 N and doped samples are the same to within ~ 0.05 eV, and we expect the 4 N bulk Fermi level to lie between these. The difference in binding energy between the doped and undoped samples in Fig. 2 must, therefore, be due to band bending in the undoped samples. Based on the extrapolation to zero photon flux, this band bending is at least 0.5 eV in the upward direction; additional non-linearity in the flux dependence would increase this value.

The measured upward band bending implies a negative surface charge on undoped β-Ga_2O_3. The STM data in Fig. 3 indicate negatively charged surface defects in UHV-annealed 4N samples. The lateral length scale is consistent with local band bending around a negatively charged defect that reduces the density of empty states available for tunneling, as seen for O interstitials in GaAs.[17] Annealing may create oxygen vacancy-interstitial pairs in the bulk; if interstitials migrate to the surface, they could then give rise to the observed negative surface charge. The derivative of the image in Fig. 3 shows continued surface corrugation through the defect,[18] consistent with interstitials embedded in the empty channels that lie directly beneath surface oxygen atoms in the β-Ga_2O_3 crystal structure.

The oxygen vacancy DFT:GGA results in Fig. 4 and Table I are consistent with recent hybrid calculations by Varley *et al.*[5] The main difference is the well-known underestimate of the band gap in the DFT:GGA calculation, which leads to the 0.32 eV activation energy for V_{O3} being a minimum estimate; it was found to be 1.2 eV in their hybrid calculation that also fits the correct 4.9 eV gap. Both calculations lead to the conclusion that oxygen vacancy defects should not contribute substantially to the carrier concentration in the bulk of β-Ga_2O_3, since the activation energy is much larger than k_bT at room temperature. This suggests that an alternate model, other than the oxygen vacancy model, for example, silicon or hydrogen doping,[4,5] is required to explain the conductivity of nominally undoped β-Ga_2O_3.

Band bending at β-Ga_2O_3 surfaces may provide an alternate explanation for the observation that annealing leads to

TABLE I. Summary of DFT:GGA calculations of formation energies of neutral and charged oxygen and gallium vacancies. Coordination number CN = number of nearest neighbors; $E^f(V^0)$ = formation energy of neutral defect. V_O takes on positive charge (donors), while V_{Ga} becomes negative (acceptors). Transition energies are referenced to the valence band maximum.

	V_{O1} ($CN=3$)	V_{O2} ($CN=4$)	V_{O3} ($CN=3$)	V_{Ga1} ($CN=4$)	V_{Ga2} ($CN=6$)
$E^f(V^0)(Ga-rich)$	1.19 eV	0.71 eV	1.43 eV	9.22 eV	9.56 eV
$E^f(V^0)(O-rich)$	4.40 eV	3.92 eV	4.64 eV	4.40 eV	4.74 eV
$\varepsilon(0/2^+)$	1.71 eV	1.10 eV	1.81 eV		
$\varepsilon(0/1^-)$				0.49 eV	0.28 eV
$\varepsilon(1^-/2^-)$				1.03 eV	0.72 eV
$\varepsilon(2^-/3^-)$				1.53 eV	1.27 eV

insulating β-Ga_2O_3 crystals. If the bands are bent up at the surface by ≥ 0.5 eV with a depletion width of several nm, it will be very difficult to make ohmic contacts to the *n*-type material, even if the bulk remains conducting. In contrast to models that attribute the conductivity decrease upon annealing in oxygen to annihilating oxygen vacancies and their associated carriers, we propose annealing leads to accumulation of negatively charged defects at the surface, either Ga vacancies or interstitial or adsorbed oxygen, causing upward band bending and failure to make an ohmic contact. We note the annealed 4N sample could support tunneling, indicative of significant bulk conduction, but a large bias was required.

Combining the DFT:GGA results with band bending results also suggests a model for gas sensing properties at β-Ga_2O_3 surfaces even in measurement geometries that are not sensitive to contact resistance (four point probe). Upward band bending comparable to $\varepsilon(2^+/0)$ would lead to near-surface de-population of the neutral of oxygen vacancies V_{O3}^0 and V_{O1}^0 in favor of doubly positive V_{O3}^{2+} and V_{O1}^{2+}, freeing electrons for some conduction mechanism. Qualitatively, this could lead to gas sensing properties at β-Ga_2O_3 surfaces.

In conclusion, based on DFT:GGA results, the activation energy of oxygen vacancy defects is too high to contribute significantly to the carrier concentration in the bulk. Based on an experimental photoemission and surface photovoltage experiment, the bands are bent upward by at least 0.5 eV at the surface of pure β-Ga_2O_3 after air-cleaving or annealing, but are flat for a highly doped crystal. Potential consequences of this upward band bending include difficulty in making ohmic contacts to *n*-type β-Ga_2O_3, which may lead to the false conclusion that the bulk crystal is insulating, and altered populations of charged vacancies in the surface region.

This work was supported by the NSF (No. DMR-0710641). The HXPS measurements were performed under the approval of NIMS Beamline Station (Proposal No. 2009A4800) with the support of HiSOR, Hiroshima University and JAEA/SPring-8. The computations were performed on a computational cluster provided by EMSL, a user facility sponsored by the DOEs Office of Biological and Environmental Research.

[1]N. Ueda, H. Hosono, R. Waseda, and H. Kawazoe, Appl. Phys. Lett. **70**, 3561 (1997).
[2]L. Binet and D. Gourier, J. Phys. Chem. Solids **59**, 1241 (1998).
[3]G. J. Exharos and X.-D. Zhou, Thin Solid Films **515**, 7025 (2007).
[4]E. G. Víllora, K. Shimamura, Y. Yoshikawa, T. Ujiie, and K. Aoki, Appl. Phys. Lett. **92**, 202120 (2008).
[5]J. B. Varley, J. R. Weber, A. Janotti, and C. G. van de Walle, Appl. Phys. Lett. **97**, 142106 (2010).
[6]M. Bartic, C.-I. Baban, H. Suzuki, M. Ogita, and M. Isai, J. Am. Ceram. Soc. **90**, 2879 (2007).
[7]P. Y. Yu and M. Cardona, *Fundamental of Semiconductors: Physics and Materials Properties* (Springer, New York, 1996).
[8]T. C. Lovejoy, E. N. Yitamben, N. Shamir, J. Morales, E. G. Villora, K. Shimamura, S. Zheng, F. S. Ohuchi, and M. A. Olmstead, Appl. Phys. Lett. **94**, 081906 (2009).
[9]G. Kresse and J. Furthmuller, Comput. Mater. Sci. **6**, 15 (1996).
[10]J. P. Perdew, J. A. Chevary, S. H. Vosko, K. A. Jackson, M. R. Pederson, D. J. Singh, and C. Fiolhais, Phys. Rev. B **46**, 6671 (1992).
[11]D. Vanderbilt, Phys. Rev. B **41**, 7892 (1990).
[12]K. Kobayashi, Nucl. Instrum. Methods Phys. Res. A **601**, 32 (2009).
[13]L. Kronik and Y. Shapira, Surf. Sci. Rep. **37**, 1 (1999).
[14]C. G. Van de Walle and J. Neugebauer, J. Appl. Phys. **95**, 3851 (2004).
[15]V. M. Bermudez, Chem. Phys. **323**, 193 (2006).
[16]K. Shimamura, E. G. Víllora, T. Ujiie, and K. Aoki, Appl. Phys. Lett. **92**, 201914 (2008).
[17]R. Wiesendanger, *Scanning Probe Microscopy and Spectroscopy: Methods and Applications* (Cambridge University Press, New York, 1994).
[18]T. C. Lovejoy, Ph.D. dissertation, Department of Physics, University of Washington, 2010.